

Pressure-Induced Charge-Order Melting and Reentrant Charge Carrier Localization in the Mixed-Valent $\text{Pb}_3\text{Rh}_7\text{O}_{15}$ *

Yan Li(李妍)¹, Zhao Sun(孙朝)¹, Jia-Wei Cai(蔡嘉伟)¹, Jian-Ping Sun(孙建平)^{2,6}, Bo-Sen Wang(王铂森)^{2,6}, Zhi-Ying Zhao(赵志颖)^{3,4}, Y. Uwatoko⁵, Jia-Qiang Yan(闫加强)³, Jin-Guang Cheng(程金光)^{2,6**}

¹College of Materials Science and Engineering, Beijing Institute of Petrochemical Technology, Beijing 102617

²Beijing National Laboratory for Condensed Matter Physics and Institute of Physics, Chinese Academy of Sciences, Beijing 100190

³Materials Science and Technology Division, Oak Ridge National Laboratory, Oak Ridge, TN 37831, USA

⁴Department of Physics and Astronomy, University of Tennessee, Knoxville, TN 37996, USA

⁵The Institute for Solid State Physics, University of Tokyo, Kashiwa, Chiba 277-8581, Japan

⁶University of Chinese Academy of Sciences, Beijing 100049

(Received 9 July 2017)

The mixed-valent $\text{Pb}_3\text{Rh}_7\text{O}_{15}$ undergoes a Verwey-type transition at $T_v \approx 180$ K, below which the development of $\text{Rh}^{3+}/\text{Rh}^{4+}$ charge order induces an abrupt conductor-to-insulator transition in resistivity. Here we investigate the effect of pressure on the Verwey-type transition of $\text{Pb}_3\text{Rh}_7\text{O}_{15}$ by measuring its electrical resistivity under hydrostatic pressures up to 8 GPa with a cubic anvil cell apparatus. We find that the application of high pressure can suppress the Verwey-type transition around 3 GPa, above which a metallic state is realized at temperatures below ~ 70 K, suggesting the melting of charge order by pressure. Interestingly, the low-temperature metallic region shrinks gradually upon further increasing pressure and disappears completely at $P > 7$ GPa, which indicates that the charge carriers in $\text{Pb}_3\text{Rh}_7\text{O}_{15}$ undergo a reentrant localization under higher pressures. We have constructed a temperature-pressure phase diagram for $\text{Pb}_3\text{Rh}_7\text{O}_{15}$ and compared to that of Fe_3O_4 , showing an archetype Verwey transition.

PACS: 72.80.Ga, 71.30.+h, 74.62.Fj

DOI: 10.1088/0256-307X/34/8/087201

As one of the most dramatic manifestations of electron correlation, the metal-insulator transition (MIT) has attracted enduring interest in the contemporary condensed matter physics.^[1,2] The charge order involving the spatial ordering of different valence states in materials is one of the most important mechanisms for MITs. In particular, the intimated interplay of charge, spin, orbital and lattice degrees of freedom in the transition metal oxides can result in complex and competing ordered ground states, which are usually fragile and thus prone to dramatic changes under some external stimuli.^[2] For example, magnetic-field induced melting of the charge-ordered antiferromagnetic insulating state in the half-doped manganite perovskites can result in the colossal magnetoresistance,^[3] while a carrier doping-induced dynamic fluctuations of charge-ordered stripes in cuprates has been considered as an important ingredient for realizing the high-temperature superconductivity.^[4] Therefore, manipulation of the charge-order-induced MIT is interesting from the viewpoints of both fundamental research and practical applications.

In this Letter, we focus on an interesting 4d-

transition-metal oxide, $\text{Pb}_3\text{Rh}_7\text{O}_{15}$, which was recently reported to undergo a charge-order-induced MIT at $T_v \approx 180$ K.^[5] It crystallizes in the hexagonal space group $P6_3/mcm$ with lattice parameters $a = 10.3537$ Å and $c = 13.2837$ Å at room temperature. The crystal structure shown in Fig. 1(a) illustrates the arrangement of the $\text{RhO}_{6/2}$ octahedra located at four different crystallographic sites (labelled as Rh1 to Rh4). As can be seen, the Rh2, Rh3, and Rh4 octahedra share edges to form a two-dimensional (2D) sheets with periodic octahedral voids; these 2D octahedral sheets are interconnected along the c axis by the face-shared Rh1 octahedral dimers via sharing common oxygens at the void positions. According to the calculations of bond valence sums above T_v , Rh1 and Rh3 are close to 3+, and Rh4 is close to 4+, whereas Rh2 is mixed-valent 3.5+. Figure 1(b) depicts the charge distribution within the 2D octahedral sheet above T_v , leading to an approximated formula of $\text{Pb}_6\text{Rh}_5^{3+}\text{Rh}_6^{3.5+}\text{Rh}_3^{4+}\text{O}_{30}$. The presence of mixed-valent Rh2 hexagonal rings renders a conducting state above T_v , featured by a weak temperature dependence of resistivity.^[5] Although it has not been decisively determined, it was proposed that the $\text{Rh}^{3.5+}$ cations

*Supported by the “Shi-Pei Ji Hua”, the National Science Foundation of China under Grant Nos 51402019 and 11574377, the Beijing Natural Science Foundation under Grant No 2152011, the National Basic Research Program of China under Grants No 2014CB921500, the Strategic Priority Research Program and Key Research Program of Frontier Sciences of the Chinese Academy of Sciences under Grant Nos XDB07020100 and QYZDB-SSW-SLH013, the U.S. Department of Energy, Office of Science, Basic Energy Sciences, Materials Sciences and Engineering Division, and the CEM, and NSF MRSEC under Grant No DMR-1420451.

**Corresponding author. Email: jgcheng@iphy.ac.cn

© 2017 Chinese Physical Society and IOP Publishing Ltd

would separate into Rh^{3+} and Rh^{4+} in an ordered fashion below T_v , giving rise to a charge-ordered state as illustrated in Fig. 1(c), which can be described as $\text{Pb}_3\text{Rh}_4^{3+}\text{Rh}_3^{4+}\text{O}_{15}$. Such a charge ordering process in $\text{Pb}_3\text{Rh}_7\text{O}_{15}$ resembles the famous Verwey transition of magnetite (Fe_3O_4) at $T_v \approx 120$ K, i.e. from $[\text{Fe}^{3+}][\text{Fe}^{2.5+}]_2\text{O}_4$ above T_v to $[\text{Fe}^{3+}][\text{Fe}^{2+}\text{Fe}^{3+}]\text{O}_4$ below T_v .^[6,7]

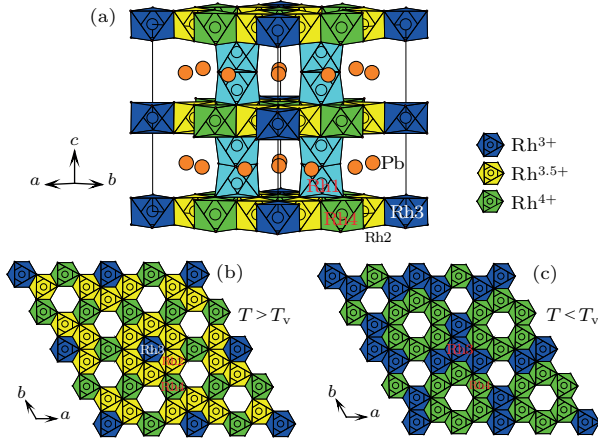


Fig. 1. (a) A schematic drawing of the crystal structure for $\text{Pb}_3\text{Rh}_7\text{O}_{15}$ having four kinds of RhO_6 octahedra displayed in different colors. The charge distributions of RhO_6 octahedra for (b) $T > T_v$ and (c) $T < T_v$.

It has been reported that the Verwey transition of Fe_3O_4 can be suppressed gradually by the application of hydrostatic pressure, leading to a metallic ground state at $P_c \sim 6$ -8 GPa.^[8] It is thus interesting to explore whether the charge-ordered insulating state in $\text{Pb}_3\text{Rh}_7\text{O}_{15}$ can be melted by high pressure as found in Fe_3O_4 . To address this question, we undertook a high-pressure study on the $\text{Pb}_3\text{Rh}_7\text{O}_{15}$ single crystal by measuring its resistivity $\rho(T)$ under various hydrostatic pressures up to 8 GPa. It is found that the application of high pressure can indeed suppress the Verwey-type transition around 3 GPa, signaling the melting of charge ordered state under pressure. However, unlike Fe_3O_4 , the metallic region above 3 GPa appears only in a limited temperature range below ~ 70 K, shrinks gradually upon further increasing pressure and disappears completely at $P \sim 7$ GPa. This result indicates that the charge carriers in $\text{Pb}_3\text{Rh}_7\text{O}_{15}$ undergo a reentrant localization under higher pressures. We have compared these results with the pressure effects on Fe_3O_4 showing the archetype Verwey transition.

Single crystals of $\text{Pb}_3\text{Rh}_7\text{O}_{15}$ used in the present study were grown out of the PbO flux according to the procedure described by Mizoguchi *et al.*^[5] Phase purity of the obtained crystals was confirmed by the powder x-ray diffraction at room temperature. Measurements of physical properties including the resistivity, magnetic susceptibility, specific heat, and Hall coefficient at ambient pressure were performed with a physical property measurement system (PPMS) and

a magnetic property measurement system (MPMS-III) from Quantum Design. The high-pressure resistivity measurements up to 8 GPa were carried out with the standard four-probe method using the Palm cubic anvil cell apparatus.^[9,10] Glycerol was employed as the pressure-transmitting medium. The pressure was calibrated at room temperature by monitoring the characteristic resistance changes of Bismuth at 2.55 and 7.7 GPa.

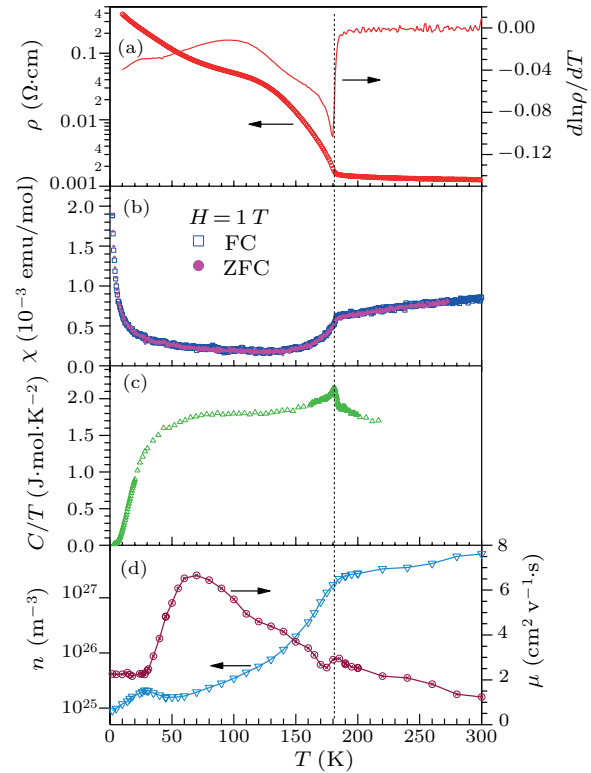


Fig. 2. Physical properties of $\text{Pb}_3\text{Rh}_7\text{O}_{15}$ single crystals: (a) in-plane resistivity $\rho(T)$ and its derivative $d \ln \rho / dT$, (b) in-plane magnetic susceptibility $\chi(T)$, (c) specific heat divided by temperature C/T , and (d) carrier density n and mobility μ derived from the Hall resistivity. The vertical dotted line indicates the transition at $T_v = 180$ K.

Figure 2 summarizes the physical properties of $\text{Pb}_3\text{Rh}_7\text{O}_{15}$ single crystal at ambient pressure. All these properties show distinct anomalies near the Verwey-type transition at $T_v \approx 180$ K, in excellent agreement with the results reported by Mizoguchi *et al.*^[5] As shown in Fig. 2(a), the resistivity $\rho(T)$ exhibits a very weak temperature dependence at $T > T_v$, and undergoes a quick increase below T_v , which can be defined clearly from the sharp peak of $d \ln \rho / dT$. The increase of $\rho(T)$ at T_v signals the opening of band gap associated with the development of charge order. However, it should be noted that the charge-ordered state of $\text{Pb}_3\text{Rh}_7\text{O}_{15}$ below T_v is not very insulating, featured by a total two-order-of magnitude increase and a relatively small $\rho(2\text{K}) \sim 0.4 \Omega\cdot\text{cm}$. In comparison, the $\rho(T)$ of Fe_3O_4 exhibits an abrupt jump by two orders of magnitude at T_v , followed by increase of more than four orders upon further de-

creasing temperatures, reaching over $10^6 \Omega\text{-cm}$ at low temperatures.^[6,8] This comparison indicates that the charge degree of freedom is not completely frozen in $\text{Pb}_3\text{Rh}_7\text{O}_{15}$, presumably due to the spatially more extended $4d$ orbitals and thus reduced coulombic repulsion.

Figure 2(b) shows the temperature dependence of magnetic susceptibility $\chi(T)$ measured under zero-field cooling (ZFC) and field-cooling (FC) modes. As can be seen, the ZFC/FC- $\chi(T)$ curves overlap with each other in the whole temperature range and experience a clear drop at T_v , which should be ascribed to the reduction of density of states due to the development of charge order. The specific heat $C(T)$ in Fig. 2(c) measured on a single-crystal sample displays a clear λ -shaped anomaly at T_v , and the absence of divergent behavior is consistent with the second-order phase transition without discernable structural changes at T_v .^[5] In comparison, the Verwey transition of Fe_3O_4 is strongly first order with a discontinuous change of $C(T)$ and a symmetry lowering structural transition at T_v .^[11]

The charge localization at T_v is further supported by our measurements of Hall effect, which was not reported in the previous study.^[5] The Hall resistivity $\rho_{xy}(H)$ curves all are linear in field with a positive slope, signaling a dominant hole carrier in the whole temperature range. Figure 2(d) shows the extracted carrier density $n = 1/R_H$ and mobility $\mu = R_H/\rho_e$, where $R_H \equiv d\rho_{xy}/dH$ is the Hall coefficient. As shown in Fig. 2(d), the carrier density n exhibits a quick reduction at T_v , while the mobility μ increases monotonically from room temperature down to ~ 70 K with only a minor anomaly at T_v . Below ~ 70 K, n changes slightly while μ exhibits a quick reduction before leveling off. These results provide us new microscopy information for understanding the electronic transport properties of $\text{Pb}_3\text{Rh}_7\text{O}_{15}$; i.e. the sudden increase of $\rho(T)$ at T_v is mainly attributed to the reduction of charge carrier due to the formation of $\text{Rh}^{3+}/\text{Rh}^{4+}$ charge order, while the further increase of $\rho(T)$ below ~ 70 K after the resistivity plateau should be ascribed to the reduced mobility.

These ambient-pressure characterizations confirm that $\text{Pb}_3\text{Rh}_7\text{O}_{15}$ undergoes a conductor-to-insulator transition at $T_v \approx 180$ K, which is attributed to the development of $\text{Rh}^{3+}/\text{Rh}^{4+}$ charge order according to the previous study.^[5] In order to check if the charge order can be melted by high pressure as observed in Fe_3O_4 , we measured the temperature dependence of resistivity $\rho(T)$ of $\text{Pb}_3\text{Rh}_7\text{O}_{15}$ single crystal under various hydrostatic pressures up to 8 GPa. Figure 3(a) shows the $\rho(T)$ curves upon warming up in the pressure range 0–3.5 GPa. As can be seen, the transition temperature T_v defined from the peak position of $d\ln\rho/dT$ moves to lower temperatures gradually with increasing pressure, reaching ~ 88 K at 3 GPa. Accompanying the decrease of T_v for $P \leq 3$ GPa, the magnitude of $\rho(T)$ below T_v decreases monotonically,

while $\rho(T)$ above T_v increases slightly and keeps a semiconducting-like temperature dependence, i.e. $d\rho/dT < 0$. When increasing pressure to 3.5 GPa, a metallic state with $d\rho/dT > 0$ is realized for $T < T_{\text{max}} \approx 70$ K, signaling the breakdown of the charge-ordered state in $\text{Pb}_3\text{Rh}_7\text{O}_{15}$. However, the metallic phase is not achieved in the whole temperature range, in contrast with the situation seen in Fe_3O_4 .^[8]

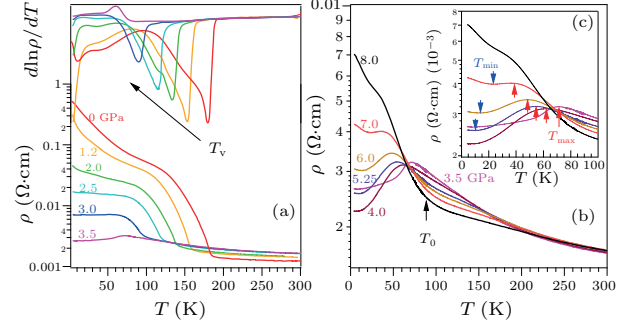


Fig. 3. High-pressure resistivity $\rho(T)$ of $\text{Pb}_3\text{Rh}_7\text{O}_{15}$ single crystal under various hydrostatic pressures: (a) 0–3.5 GPa, (b) 3.5–8 GPa. The transition temperatures at T_v below 3.5 GPa are determined from the peak of $d\ln\rho/dT$ as shown in the top panel of (a). An enlarged view in (c) marks the evolution of the resistivity maximum T_{max} (up-pointing arrows) and minimum T_{min} (down-pointing arrows) as a function of pressure.

Upon further increasing pressure to above 3.5 GPa, the resistivity peak position at T_{max} shifts gradually to lower temperatures as shown by the up-pointing arrows in Fig. 3(c). Interestingly, the magnitude of $\rho(T)$ for $T < T_{\text{max}}$ increases again with pressure, and an upturn develops below a T_{min} , which moves up with pressure for $P > 4$ GPa and results in a gradual shrink of the metallic phase between T_{max} and T_{min} . Eventually, the metallic region disappears completely at 8 GPa. Meanwhile, a clear reduction of $\rho(T)$ at $T > T_{\text{max}}$ is also evidenced in Fig. 3(b), leading to a slope change of $\rho(T)$ at $T_0 \sim 80$ –90 K as indicated by the arrow. These results imply that the charge carriers in $\text{Pb}_3\text{Rh}_7\text{O}_{15}$ undergo a reentrant localization under higher pressures.

The characteristic temperatures T_v , T_{max} , T_{min} and T_0 determined from the above $\rho(T)$ data are plotted in Fig. 4 as a function of pressure. A contour plot of all the $\rho(T)$ data is also superimposed in Fig. 4 to illustrate the characteristic changes of resistivity in different pressure ranges. As can be seen, the Verwey-type transition at T_v is suppressed gradually by pressure and disappears around 3 GPa, above which a metallic region ($d\rho/dT > 0$) emerges in a limited temperature range. The confined metallic phase between T_{max} and T_{min} shrinks with pressure and vanishes completely at ~ 7 GPa. The $\rho(T)$ curves at 7–8 GPa exhibit an enhancement below T_0 . Thus, the temperature-pressure phase diagram of $\text{Pb}_3\text{Rh}_7\text{O}_{15}$ is featured by a melting of charge-ordered insulating state around 3 GPa and a reentrant charge localization

above 7 GPa with a confined metallic phase between them.

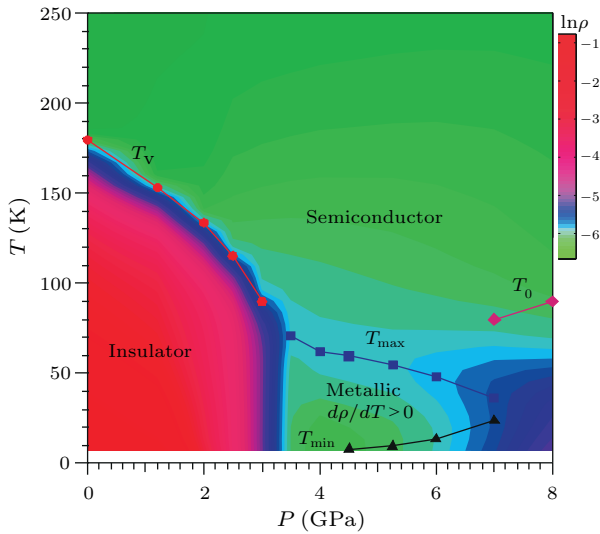


Fig. 4. Temperature-pressure phase diagram of $\text{Pb}_3\text{Rh}_7\text{O}_{15}$ based on the high-pressure resistivity measurements.

This present work is the first study attempting to clarify the hydrostatic pressure effects on the $\text{Pb}_3\text{Rh}_7\text{O}_{15}$ with a Verwey-type transition as Fe_3O_4 . Thus, it is instructive to compare the effects of pressure on $\text{Pb}_3\text{Rh}_7\text{O}_{15}$ with that of Fe_3O_4 . (i) T_v versus P : Although the former has a higher T_v than the latter, the charge-ordered state below T_v in $\text{Pb}_3\text{Rh}_7\text{O}_{15}$ is not as insulating as that of Fe_3O_4 as mentioned above. The critical pressure $P_c \approx 3$ GPa for melting the charge-ordered insulating phase in $\text{Pb}_3\text{Rh}_7\text{O}_{15}$ is about half of the $P_c \approx 6-8$ GPa for Fe_3O_4 . These differences may originate from the distinct orbital characters, i.e. $4d$ versus $3d$; the larger spatial extension of the $4d$ orbitals makes it relatively easier to destabilize the charge ordered state in $\text{Pb}_3\text{Rh}_7\text{O}_{15}$. (ii) *The pressure-induced metallic state*: After the melting of the charge-ordered state above P_c , the metallic state in $\text{Pb}_3\text{Rh}_7\text{O}_{15}$ appears only in a confined temperature and pressure range, and is destabilized under higher pressures. In contrast, the metallic ground state is realized above P_c in the whole temperature range for Fe_3O_4 . Such a difference arises from the opposite response to pressure of the semiconducting state above T_v . (iii) *The semiconducting state above T_v* : Despite of a less insulating state below T_v , the semiconducting states above T_v in $\text{Pb}_3\text{Rh}_7\text{O}_{15}$ is very robust against pressure. As illustrated in Fig. 3(a), the $\rho(T)$ of $\text{Pb}_3\text{Rh}_7\text{O}_{15}$ at $T > T_v$ actually increases with pressure and the semiconducting-like behavior persists in the whole investigated pressure range. In sharp contrast, the $\rho(T)$ of Fe_3O_4 at $T > T_v$ decreases monotonically with pressure, and changes from semiconducting-like to metallic at lower pressures than P_c . (iv) *The reentrant charge carrier localization under higher pres-*

sure: The robustness of the semiconducting state in $\text{Pb}_3\text{Rh}_7\text{O}_{15}$ should connect with the diminishing of the metallic phase and the reentrant charge localization under higher pressures. In a recent high-pressure study on Fe_3O_4 , a reentrant insulating behavior is observed at $P > 23$ GPa, which has been attributed to the pressure-induced structural transition from the cubic to an orthorhombic phase.^[12] Whether there exists a pressure-induced structural transition in $\text{Pb}_3\text{Rh}_7\text{O}_{15}$ deserves further studies.

In summary, we have grown the $\text{Pb}_3\text{Rh}_7\text{O}_{15}$ single crystal with the flux method and characterized its physical properties at ambient pressure. Our new Hall data provide microscopic evidences for the reduction of charge carrier at $T_v \approx 180$ K due to the development of the Verwey-type $\text{Rh}^{3+}/\text{Rh}^{4+}$ charge ordering. We further investigate the effect of pressure on the Verwey-type transition of $\text{Pb}_3\text{Rh}_7\text{O}_{15}$ by measuring its resistivity under hydrostatic pressures up to 8 GPa. We find that the Verwey transition can be suppressed around 3 GPa, above which the charge-ordered insulating state is melted to a metallic state below ~ 70 K. However, the low-temperature metallic region shrinks gradually upon further increasing pressure and disappears completely at $P > 7$ GPa, which indicate that the charge carriers in $\text{Pb}_3\text{Rh}_7\text{O}_{15}$ undergo a reentrant localization under higher pressures. A side-by-side comparison between $\text{Pb}_3\text{Rh}_7\text{O}_{15}$ and Fe_3O_4 highlights that the different $4d$ versus $3d$ orbital characters may be responsible for the distinct responses to external pressure in these two compounds. A high-pressure structural study on $\text{Pb}_3\text{Rh}_7\text{O}_{15}$ is needed to further understand the reentrant charge carrier localization under higher pressures.

References

- [1] Mott N 1984 *Rep. Prog. Phys.* **47** 909
- [2] Imada M, Fujimori A and Tokura Y 1998 *Rev. Mod. Phys.* **70** 1039
- [3] Dagotto E, Hotta T and Moreo A 2001 *Phys. Rep.* **344** 1
- [4] Salkola M I, Emery V J and Kivelson S A 1996 *Phys. Rev. Lett.* **77** 155
- [5] Mizoguchi H, Ramirez A P, Siegrist T, Zakharov L N, Sleight A W and Subramanian M A 2009 *Chem. Mater.* **21** 2300
- [6] Verwey E J W 1939 *Nature* **144** 327
- [7] Wright J P, Attfield J P and Radaelli P G 2001 *Phys. Rev. Lett.* **87** 266401
- [8] Mori N, Todo S, Takeshita N, Mori T and Akishige Y 2002 *Physica B* **312-313** 686
- [9] Uwatoko Y, Matsubayashi K, Matsumoto T, Aso N, Nishi M, Fujiwara T, Hedo M, Tabata S, Takagi K, Tado M and Kagi H 2008 *Rev. High Press. Sci. Technol.* **18** 230
- [10] Cheng J G, Matsubayashi K, Nagasaki S, Hisada A, Hirayama T, Hedo M, Kagi H and Uwatoko Y 2014 *Rev. Sci. Instrum.* **85** 093907
- [11] Walz F 2002 *J. Phys.: Condens. Matter* **14** R285
- [12] Muramatsu T, Gasparov L V, Berger H, Hemley R J and Struzhkin V V 2016 *J. Appl. Phys.* **119** 135903